euspen's 22nd International Conference & Exhibition, Geneva, CH, May/June 2022
www.euspen.eu

Adjustable stiffness compensation for monolithic high-precision mechanisms

Mario André Torres Melgarejo, Martin Wittke, René Theska

Technische Universität Ilmenau, Department of Mechanical Engineering
Institute for Design and Precision Engineering, Precision Engineering Group

E-mail: mario.torres@tu-ilmenau.de

Abstract
Compliant mechanisms are widely used in precision engineering and metrology due to their numerous advantageous properties, such as high accuracy and high repeatability. In some applications, especially in force and mass measurement technologies, the restoring forces of the compliant elements have a negative effect on the desired system properties. To compensate for the positive stiffness, elements with negative stiffness such as preloaded springs or buckled leaf springs are typically integrated. Most existing approaches are, however, either non-monolithic, difficult to readjust, and/or can introduce parasitic forces into the main mechanism, limiting their use for highest-precision applications. The following contribution presents a compliant mechanism with adjustable negative stiffness, which can be easily integrated into the main mechanism with minimum parasitic effects. The negative stiffness is achieved here by preloading a flexure spring element. By means of a lever sub-mechanism and a coupling element, the compensation force is transmitted to the main mechanism while decoupling its parasitic component. The embodiment design uses the high tensile stiffness of the flexure hinges conveniently to support the relatively large preloading force while avoiding buckling. The present paper focuses on the functioning of the compensation mechanism, a validation through kinetic and finite element analysis as well as its application in a monolithic precision guiding mechanism.

Keywords: stiffness compensation, compliant mechanism, adjustable stiffness, monolithic design

1. Introduction

In compliant mechanisms, the elastic deformation of material-coherent joints is purposely used to generate motion. Solid friction and backlash are avoided, resulting in high repeatability. An appropriate kinematic design allows for high accuracy of the intended motion. Suitability for monolithic manufacturing eliminates the need for assembly, reducing geometric deviations. As a result, compliant mechanisms find many applications in precision engineering [1] and metrology [2].

The intrinsic restoring forces of the deformation or „stiffness“ may represent a limiting factor depending on the application. In force and mass measurement systems, the stiffness of the deformation body limits the achievable measurement resolution [3]. In positioning systems, stiff flexure guides put high demands on the design of the actuation units. To compensate for the „positive“ stiffness, a counteraction increasing along the direction of motion is required, i.e. „negative“ stiffness. Many approaches to produce compensation have been proposed, including trim masses [2], preloaded springs [4], and buckled leaf springs [5]. However, such methods bring alongside effects not compatible with the highest demands on precision. Among these are parasitic forces, a non-monolithic layout, as well as the lack or complexity of readjustment.

The following contribution introduces a novel compliant mechanism to be used for stiffness compensation. The negative stiffness can be easily achieved and adjusted by preloading a flexure spring element. Monolithic integration within the main compliant mechanism can be achieved with minimum parasitic effects. The working principle of the compensation mechanism is thoroughly explained and validated using different modelling approaches as well as in an application example.

2. Adjustable stiffness compensation mechanism

A rigid-body model of the stiffness compensation mechanism is presented in Fig. 1a. The mechanism is composed of a tensile spring (1) of stiffness C_s pivoted at joint A and connected to a lever (2) at joint C. The lever is then connected to the main mechanism of stiffness C_m at joint E by the coupling element (3).

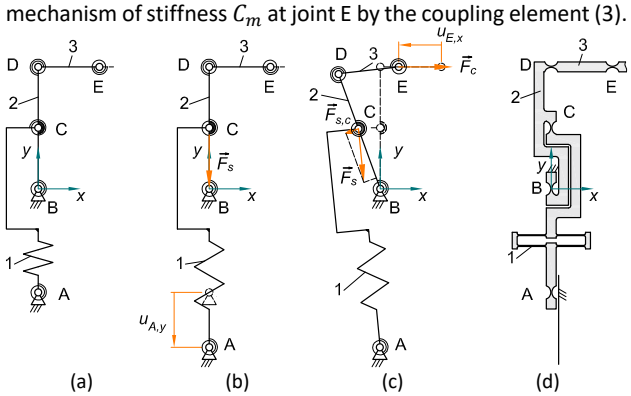

Figure 1. Stiffness compensation compliant mechanism: (a) rigid-body model in initial non-deflected state, (b) rigid-body model in preloaded non-deflected state, (c) rigid-body model in preloaded deflected state, (d) embodiment design based on arbitrary flexure hinges.

The negative stiffness is achieved by displacing joint A along the *y*-axis (see Fig. 1b) and, thus, preloading the tensile spring (1) with a force $F_s = C_s \cdot u_{A,y}$. In the non-deflected state, the preload force is mainly supported by the lever element (2) and is not transmitted to the main mechanism as a purely parasitic force. Parasitic forces in the *y*-direction are minimized by the coupling element (3). During deflection (see Fig. 1c), the component $F_{s,c}$ of the preload force F_s acting in the direction of motion is transmitted to the main mechanism through the lever

(2) and a coupling element (3). The resulting force at joint E is defined as the compensation force F_c (see Equation 1).

$$F_c(u_{E,x}) = F_{s,c}(C_s, u_{A,y}, u_{E,x}) \cdot \frac{\overline{BC}}{\overline{BE}} - C_c(u_{A,y}) \cdot u_{E,x}, \quad (1)$$

where $C_c(u_{A,y})$ is the stiffness of the compensation mechanism with joint A displaced but the tensile spring without preload. To compensate for the stiffness of the main mechanism C_m, a preload force F_s is required so that $F_c \approx C_m \cdot u_{E,x}$. This can be achieved by adjusting $u_{A,y}$ for a given value of C_s.

A compliant mechanism based on the rigid-body model is designed by replacing the revolute joints with flexure hinges [6], see Fig. 1d. The tensile spring (1) is replaced by a flexure spring element with distributed compliances. To avoid parasitic deformations as well as buckling, the hinges are oriented making use of their high tensile stiffness to support the preload force.

3. Concept validation

To validate the concept, the stiffness characteristic curve of the mechanism is investigated using a rigid-body model as well as a 3D finite element model. Table 1 shows the parameters used. The stiffnesses of the torsion springs on the revolute joints and the tensile spring are equally deployed for both models. To maximize motion accuracy with regard to the rigid-body model, semi-circular flexure hinges are used. Local mesh refinements in the compliant elements were also performed. The calculations are done in two steps. First, the preloading $u_{A,y}$ is introduced while the displacement of joint E $u_{E,x}$ is zero. Then, joint E is displaced and the force reaction F_c is evaluated.

Table 1 Parameters of investigated stiffness compensation mechanism

Parameter	Value	Parameter	Value
Joint stiffness	101.8 Nmm/rad	$\overline{AB}, \overline{BC}, \overline{CD}$	40 mm
Spring stiffness	37,7 N/mm	$\overline{DE}$	20 mm

Fig. 2 shows the stiffness characteristic curve for different preloading positions $u_{A,y}$. For the investigated configuration, a nearly zero actuation force F_C and, thus, a nearly zero average stiffness is attained with $u_{A,y} = 0.346$ mm in both models. By adjusting past this value, the mechanism acquires a negative stiffness and can be used for compensation. The results also show good agreement between both models for small deflections (< 1 mm) of the coupling point E.

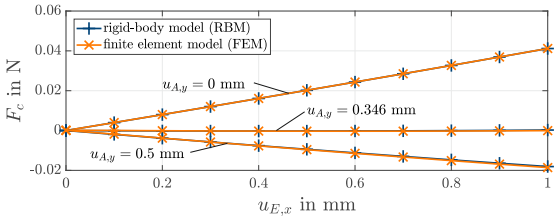

Figure 2. Stiffness characteristic curve of the compensation mechanism.

4. Application on a guiding mechanism

Fig. 3 shows a monolithic linear guiding mechanism with the integrated stiffness compensation. The flexure hinges of the guiding mechanism are identical to those of the compensation mechanism in Section 3. Lengths $\overline{FG}$ and $\overline{HI}$ equal to 100 mm, while $\overline{FH}$ and $\overline{GI}$ equal to 80 mm.

Using the same modelling approaches as in Section 3, the stiffness characteristic curve is determined, see Fig. 4. The results of the rigid-body and finite element models are in good accordance. With the compensation mechanism at zero average stiffness ($u_{A,y} = 0.346$ mm), the resulting characteristic curve is similar to that of the original guiding mechanism. With a preload position of $\Delta u_{A,y} = 0.870$ mm, the actuation force F_x can be reduced to a value of almost zero (< 2 mN).

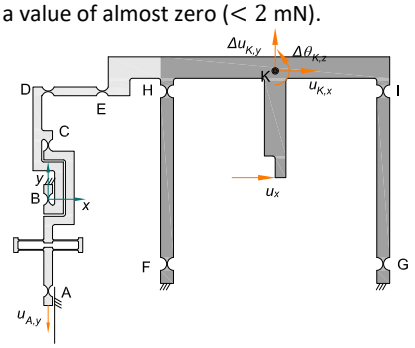

Figure 3. Monolithic guiding mechanism with stiffness compensation.

The parasitic effect of the stiffness compensation on the motion behavior of the guiding mechanism is also evaluated using the 3D finite element model. The guiding deviation $\Delta u_{K,y}$ at the coupling point K with and without compensation equals to 6.21 µm and 6.22 µm, respectively. Thus, the parasitic effect of the compensation can be considered neglectable.

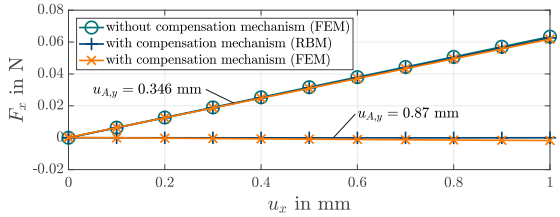

Figure 4. Stiffness characteristic curve of the guiding mechanism.

5. Summary

This paper presents an adjustable stiffness compensation mechanism that can be integrated into a compliant mechanism with minimum side effects. The working principle is explained and validated using rigid-body and finite element models. A first embodiment design and its application in a flexure guiding mechanism are also investigated. A reduction of the actuation force from >60 mN to <2 mN was achieved with an adjustment resolution of 1 µm. The influence on the maximum guiding deviation amounts to 0.16 %, which is considered neglectable.

The presented stiffness compensation principle shows great potential to be used in highly sensitive mechanisms, where compensation forces often introduce parasitic effects. Simplified analytical equations for the straightforward design of the compensation mechanism as well as design guidelines represent the current research work. Investigation of the characteristic curve around zero average stiffness, experimental verification of the simulations on prototypes as well as further optimization of the compliant mechanism design are also future work.

Acknowledgments

The authors thank the German Research Foundation (DFG) for the financial support of the project with Grant No. TH 845/9-1.

References

[1] Theska R, Zentner L, Fröhlich T, Weber C, Manske E, Linß S, Gräser P, Harfensteller F, Darnierder M and Kühnel M 2019 *Mechanisms and Machine Science* **71** 249-256

[2] Darnieder M, Pabst M, Wenig R, Zentner L, Theska R and Fröhlich T 2018 *J. Sens. Sens. Syst.* **7** 587-600

[3] Speake C C 1987 *Proc. R. Soc.* A **414** 333-358

[4] Consadier F, Henein S, Richard M and Rubbert L 2017 *The art of flexure mechanism design*

[5] Gallego Sanchez J A and Herder J L 2013 *13th World Congress in Mechanism and Machine Science* A23_545

[6] Linß S, Gräser P, Henning S, Harfensteller F, Theska R and Zentner L 2019 *Mechanisms and Machine Science* **73** 1569-1578